Pressure Distribution on a Rectangular Wing with a Jet Exhausting Normally into an Airstream

P. T. Wooler,* G. H. Burghart,† and J. T. Gallagher‡
Northrop Corporation, Norair Division, Hawthorne, Calif.

The interaction between a jet exhausting normally from a lifting surface into a uniform airstream is explored theoretically and experimentally. A theoretical model of the flow is discussed in which the entrainment of the mainstream fluid by the jet is accounted for directly, without recourse to an empirical equation for the jet centerline. Making use of the observation that the jet deforms from a circular cross section into an elliptical cross section as it progresses downstream, the continuity and momentum equations are solved to provide the jet path. The velocity field induced by the jet is then determined by replacing the jet by a sink-doublet distribution. The distribution of sinks represents the entrainment effect of the jet, and the doublet distribution represents the blockage effect of the jet. Lifting surface theory is used to predict the loading on the adjacent lifting surface. The theory does account for the three-dimensionality of the problem, and there is good agreement between theory and the results of an experiment conducted on a 10% thick straight wing at $AR = 3$.

Nomenclature

A = loading coefficient matrix
A_j = jet cross-sectional area
AR = aspect ratio
b = wing span
c = wing chord
C = circumference of jet cross section
C_D = crossflow drag coefficient of jet
C_p = pressuse coefficient
d = length of major axis in elliptical representation of jet cross section
D = influence matrix
D^T = transpose of D
E_1,E_2,E_3 = entrainment coefficients
K = influence function
m = velocity ratio U_{j0}/U
$\bar{m}$ = sink strength of jet element/unit length in η direction
P = reference point
P^1 = orthogonal projection of P on the $Z = 0$ plane
R = local jet radius of curvature
s = coordinate along jet centerline
S = wing surface area
T = thrust of jet
U = mainstream speed
U_j = jet speed
u_1,v_1,w_1 = induced velocities in the ξ, η, ζ directions due to a doublet
u_s,v_s,w_s = induced velocities in the X,Y,Z directions due to sink distribution
u_B,v_B,w_B = induced velocities in the X,Y,Z directions due to doublet distribution
u,v,w = induced velocity in the X,Y,Z directions due to sink plus doublet distributions
W = downwash matrix
X,Y,Z = coordinate system defined in Fig. 1
X_c,Y_c = X,Y coordinates of a downwash control point
ΔC_P = wing loading
δs = increment of arc of jet centerline
θ = angle defined in Fig. 1
μ = doublet strength
ρ = density of jet and mainstream fluids

Subscripts

0 = conditions at the jet exit
p = reference point

Superscripts

* = nondimensional value
′ = first derivative with respect to z
″ = second derivative with respect to z

Presented as Paper 67-1 at the AIAA 5th Aerospace Sciences Meeting, New York, January 23–26, 1967; submitted January 19, 1967; revision received June 23, 1967. [3.02]

* Engineering Specialist, Research and Technology; now with University of Salford, Lancashire, England.

† Engineer, Research and Technology Section; now with TRW Systems. Member AIAA.

‡ Member of Technical Management, Research and Technology Section.

Introduction

THERE is considerable interest in airplanes with the capability of taking off and landing in a short distance. One method of achieving such performance is to use lifting jets or fans installed in the wing or fuselage of the airplane which exhaust at right angles to the direction of flight.

In the transition phase of such flight, important jet on airstream interference problems arise. It has been demonstrated experimentally that in the transition phase the jet induces asymmetric pressure loading on the surface from which it is exhausting. The pressure loading can adversely affect the lift and pitching moments on the airplane. The development of a satisfactory theoretical model of this type of flowfield is therefore desirable to assist in the design of V/STOL airplanes, and to enable a satisfactory wind-tunnel correction method to be developed for powered lift wind-tunnel testing.

A number of people have experimentally studied the flowfields in the vicinity of the jet exhausting from a surface.[1–4] There has been very little theoretical work published to date,[5–7] and a satisfactory model of the flow has not been put forward. An extensive theoretical treatment has been made by Monical.[8] He reduces an empirical equation for jet centerlines, and then replaces the jet by a vortex lattice flared at the downstream end to simulate flow in the jet. The assumption of the path location and the lack of entrainment effects, however, limit the effectiveness of the method as a theoretical model.

In this paper, a model is suggested which includes the entrainment of the mainstream fluid in the analysis. After making certain assumptions, based on experimental observation of the jet geometry, the equations of motion determining the growth and displacement of the jet are solved numerically. With a suitable choice of the entrainment parameters, the calculation of the jet centerline is in good agreement with experimental results. The interference effects between the

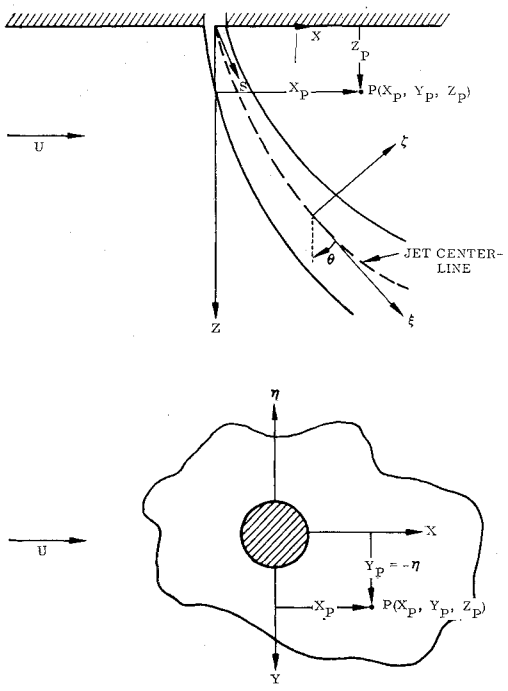

Fig. 1 Coordinate systems.

jet and the lifting surface are accounted for by distributing sinks and doublets along the jet. The sink strengths are made proportional to the mass of air entrained, and the doublet strengths are such as to represent the blockage effects of the jet. From this distribution of sinks and doublets the downwash field induced at the lifting surface is predicted. By treating the downwash distribution as an effective surface camber, it is possible to use lifting surface theory to predict the induced pressure distribution on the wing. It is also possible to account for the induced flow parallel to the wing by altering the freestream-induced component by the amount predicted from the sink doublet distribution. This permits the effects of the jet on the loading distribution to be computed, and the predicted loadings are shown to be in good agreement with experimental results.

Equations of Motion

When a jet exhausts at an angle into a uniform mainstream, it is deflected partly by viscous entrainment and partly by pressure forces on the jet boundary. It is assumed that the flow is incompressible and nonviscous except that viscosity is the mechanism that causes entrainment; then dimensional considerations suggest that the entrainment of mainstream fluid into unit length of the jet may be written

$$E = \rho E_1 U d \cos\theta + \frac{\rho E_2 (U_j - U \sin\theta) C}{1 + E_3 U \cos\theta / U_j} \tag{1}$$

A fluid particle approaching the jet and near the plane of symmetry will be more easily entrained by the jet than a particle that is moving away from the jet. The susceptibility of the approaching particles to jet entrainment is accounted for by the term $E_1 U d \cos\theta$ in expression (1). Particles moving away from the jet or to its side with momentum not directed towards the jet are less tolerant to jet entrainment. The term

$$\frac{\rho E_2 (U_j - U \sin\theta) C}{1 + E_3 U \cos\theta / U_j}$$

takes this into consideration while satisfying the Ricou-Spalding solution for the freejet case when $U = 0$.

The pressure force acting on a jet element of unit length is

$$C_D \cdot \tfrac{1}{2}\rho U^2 \cos^2\theta d \tag{2}$$

C_D being the crossflow drag coefficient of the jet.

The equations of motion can now be written using the coordinate system defined in Fig. 1.

Equation of Continuity

$$\rho (d/ds)(A_j U_j) = E \tag{3}$$

Momentum Equation

$$\rho (d/ds)(A_j U_j^2) = EU \sin\theta \tag{4}$$

Force Equation

$$\begin{aligned} \rho A_j U_j^2 / R &= EU \cos\theta + C_D \tfrac{1}{2}\rho U^2 \cos^2\theta d \\ &= \rho A_j U_j^2 X'' / [1 + (X')^2]^{3/2} \end{aligned} \tag{5}$$

Replacing d/ds by $\cos\theta (d/dZ)$ in Eqs. (3) and (4) reduces the problem to one of finding d, U_j, and X as functions of Z and the parameters E_1, E_2, E_3, and C_D. To do this, it is necessary to establish the functional relationships $A_j[d(Z)]$ and $C[d(Z)]$ from the geometry of the jet growth.

Experimental observations[1] show that there is a region in which the jet deforms from its initial circular cross section into a kidney-shaped one. Reference 3 points out that once this shape is attained, the jet cross section remains relatively similar in shape. It did not appear possible to account for the exact jet shape and the trailing vortices which control it, so a simplified jet shape, an ellipse, was selected. Experimental data[6] indicate that the initial growth of the jet is approximately linear; and correlations of data have indicated that the extent of the region in which the jet shape is deforming is a function of the jet exit to mainstream velocity ratio U_{j0}/U. This may be written $0 \leq ZU/d_0 U_{j0} \leq 0.3$ when $Z/d_0 \geq 0.3\ U_{j0}/U$ observations show that the best fit of the jet cross section with an ellipse is one with a ratio of minor to major axis of $\frac{1}{4}$. Therefore, the geometry of the jet was treated in two regions:

1) A region in which the jet has an elliptical cross section and the ratio of minor to major axis decreases linearly from 1 at $Z/d_0 = 0$ to $\frac{1}{4}$ at $Z/d_0 = 0.3 U_{j0}/U$. Thus, we have

$$\text{minor axis/major axis} = 1 - [\tfrac{5}{2}(Z/d_0)(U/U_{j0})]$$

$$C = \pi d \left(\frac{1 + [1 - \frac{5}{2}(Z/d_0)(U/U_{j0})]^2}{2} \right)^{1/2}$$

$$0 \leq \frac{Z}{d_0}\frac{U}{U_{j0}} \leq 0.3 \tag{6}$$

$$A_j = \pi \left(1 - \frac{5}{2}\frac{Z}{d_0}\frac{U}{U_{j0}} \right) \frac{d^2}{4}$$

From the preceding expressions it is seen that for a given nonzero jet exit velocity as $U \to 0$ the development region becomes $0 \leq Z/d_0 \leq \infty$ and the jet retains its circular cross section, which is to be expected since the jet is then exhausting into quiescent surroundings.

2) A region in which the jet retains a similar elliptical cross section with

$$\left.\begin{aligned} \text{minor axis/major axis} &= \tfrac{1}{4} \\ C &= 2.24d \\ A_j &= \pi d^2/16 \end{aligned}\right\} \qquad \frac{Z}{d_0}\cdot\frac{U}{U_{j0}} \geq 0.3 \tag{7}$$

Integration of the Equations of Motion

Substituting the geometric parameters from expressions (6) and (7) into Eqs. (3–5) the nondimensional form of these

equations is easily obtained. The equations become

$$\frac{dU_j^*}{dZ^*} = \left[E_1\cos\theta + \frac{E_2}{1 + E_3\cos\theta/U_j^*m} \times (mU_j^* - \sin\theta)\pi\left(\frac{1 + [1 - \frac{5}{2}(Z^*/m)]^2}{2}\right)^{1/2}\right] \times \left[\frac{\sin\theta - mU_j^*}{[(\pi/4)(1 - \frac{5}{2}(Z^*/m)]d^*m^2U_j^*\cos\theta}\right] \quad (8)$$

$$\frac{dd^*}{dZ^*} = \left\{\left[E_1\cos\theta + \frac{E_2}{1 + E_3\cos\theta/U_j^*m}(mU_j^* - \sin\theta)\pi \times \left(\frac{1 + [1 - \frac{5}{2}(Z^*/m)]^2}{2}\right)^{1/2}\right]\frac{d^*}{m\cos\theta} + \frac{5}{8}\pi\frac{d^{*2}U_j^*}{m} - \frac{\pi}{4}d^{*2}\left(1 - \frac{5}{2}\frac{Z^*}{m}\right)\frac{dU_j^*}{dZ^*}\right\} \Big/ \frac{\pi d^*U_j^*}{2}\left(1 - \frac{5}{2}\frac{Z^*}{m}\right) \quad (9)$$

$$\frac{d^2X^*}{dZ^{*2}} = \left[1 + \left(\frac{dX^*}{dZ^*}\right)^2\right]^{3/2}\left[\frac{(E_1 + 0.5C_D)\cos\theta + \frac{E_2}{1 + E_3\cos\theta/U_j^*m}(mU_j^* - \sin\theta)\pi\left(\frac{1 + [1 - \frac{5}{2}(Z^*/m)]^2}{2}\right)^{1/2}}{m^2(\pi/4)d^*U_j^{*2}[1 - \frac{5}{2}(Z^*/m)]}\right]\cos\theta \quad (10)$$

$$\frac{dU_j^*}{dZ^*} = \frac{16}{\pi m^2 d^* U_j^*\cos\theta}\left[E_1\cos\theta + \frac{E_2}{1 + E_3\cos\theta/U_j^*m}(mU_j^* - \sin\theta)2.24\right][\sin\theta - mU^*] \quad (11)$$

$$\frac{dd^*}{dZ^*} = \frac{E_1\cos\theta + \frac{E_2}{1 + E_3\cos\theta/U_j^*m}(mU_j^* - \sin\theta)2.24 - \frac{\pi}{16}m\cos\theta d^*\frac{dU_j^*}{dZ^*}}{(\pi/8)m\cos\theta U_j^*} \quad (12)$$

$$\frac{d^2X^*}{dZ^{*2}} = \frac{16\cos\theta}{\pi m^2 d^* U_j^{*2}}\left[1 + \left(\frac{dX^*}{dZ^*}\right)^2\right]^{3/2}\left[(E_1 + 0.5C_D)\cos\theta + \frac{E_2}{1 + E_3\cos\theta/U_j^*m}(mU_j^* - \sin\theta)\,2.24\right] \quad (13)$$

Equations (8–10) are to be used when $0 \leq Z^*/m \leq 0.3$ and Eqs. (11–13) are to be used when $Z^*/m > 0.3$.

Writing

$$\cos\theta = \frac{1}{[1 + (dX^*/dZ^*)^2]^{1/2}}$$

$$\sin\theta = \frac{dX^*/dZ^*}{[1 + (dX^*/dZ^*)^2]^{1/2}}$$

we see that the preceding group of equations represents a set of differential equations to be solved for U_j^*, d^*, X^* as functions of Z^* and the parameters E_1, E_2, E_3, and C_D. It has not been possible to integrate these equations in closed form, but they have been integrated numerically with the aid of a digital computer using a Taylor series expansion method.

It was necessary, prior to the integration, to establish values for the parameters E_1, E_2, E_3, and C_D. E_2 was determined by considering results for a freejet.[8] When $U = 0$, Eqs. (3) and (4) reduce to

$$(d/dZ)(A_jU_j) = E_2U_jC \quad (14)$$

$$(d/dZ)(A_jU_j^2) = 0 \quad (15)$$

$$C = \pi d \quad (16)$$

$$A_j = \pi d^2/4 \quad (17)$$

It is easily seen that Eqs. (14–17) imply

$$dd/dZ = 4E_2$$

so that

$$\frac{1}{A_{j0}U_{j0}}\frac{d(A_jU_j)}{d(Z/d_0)} = 4E_2$$

Ricou and Spalding[9] have measured the entrainment by the freejet and showed that the rate of change of the integrated jet momentum with distance along the jet was constant and equal to 0.32. Then, to get the correct development of the jet when $U = 0$, E_2 must be set equal to 0.08.

The drag coefficient C_D for the jet was obtained by assuming the jet was a solid, elliptical cylinder with a $C_D = 1.8$. With these values of E_2 and C_D, the equations were integrated for a number of different values of E_1 and E_3. E_1 and E_3 were finally chosen at the values giving good correlation between experimental and theoretically determined jet centerlines, as shown on Fig. 2.

The final set of parameters used in the integration was $E_1 = 0.35$, $E_2 = 0.08$, $E_3 = 30$, $C_D = 1.8$.

Calculation of the Velocity Field

To get the jet interference velocity field, the entrainment of mainstream fluid into the jet is replaced by a uniform sink distribution along the jet axis normal to the oncoming mainstream (Fig. 3). The integrated strength of this sink distribution is given by expression (1).

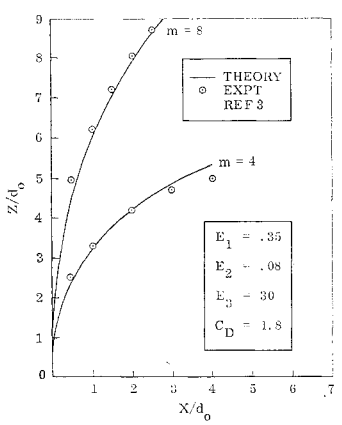

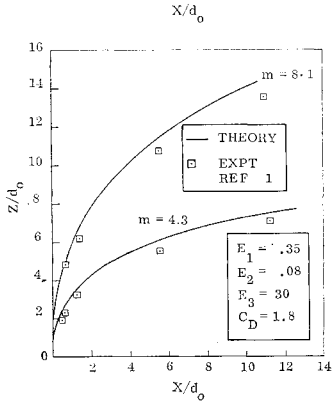

Fig. 2 Jet centerlines.

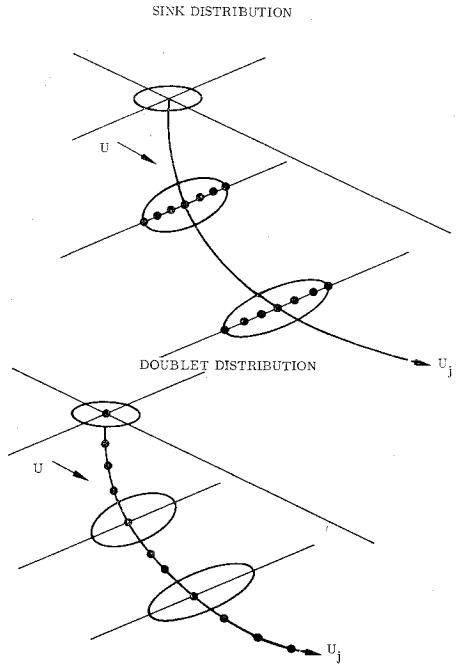

Fig. 3 Sink and doublet distributions on jet path.

The blockage effect of the jet is represented by a doublet distribution along the jet centerline (Fig. 3). The strength of this distribution of doublets is obtained from the coefficient of the $1/z$ term in the complex velocity potential expansion $W(z)$ for the two-dimensional flow past an ellipse as presented in Ref. 10. By replacing the jet with a doublet distribution, we are effectively considering the flow past an equivalent circular cylinder. Thus, near the jet itself we do not expect to get good representation of the flow, although this could be improved by including more terms of the expansion.

Consider an element of the jet, length δs, centered at $(X,0,Z)$. The sink strength/unit distance in the η direction will then be given by

$$\bar{m} = \left[E_1 U d \cos\theta + \frac{E_2}{1 + E_3 U \cos\theta/U_j}(U_j - U \sin\theta)C\right]\frac{\delta s}{d} \tag{18}$$

With the help of Fig. 1 we see that the induced velocity at a point $P(X_p,Y_p,Z_p)$ due to a sink element of length $\delta\eta$ will be

$$\frac{\bar{m}\, d\eta}{4\pi[(Z - Z_p)^2 + (X - X_p)^2 + (Y_p + \eta)^2]} \tag{19}$$

The induced velocities in the direction of the axes X, Y, Z are then seen to be

$$\frac{\bar{m}d\eta(X - X_p)}{4\pi[(Z - Z_p)^2 + (X - X_p)^2 + (Y_p + \eta)^2]^{3/2}}$$

$$- \frac{\bar{m}d\eta(Y_p + \eta)}{4\pi[(Z - Z_p)^2 + (X - X_p)^2 + (Y_p + \eta)^2]^{3/2}}$$

and

$$\frac{\bar{m}d\eta(Z - Z_p)}{4\pi[(Z - Z_p)^2 + (X - X_p)^2 + (Y_p + \eta)^2]^{3/2}}$$

respectively.

Integration of the preceding expressions over the range $d/2 \leq \eta \leq d/2$ results in the following equations for the induced velocities δu_s, δv_s, δw_s at P due to the sink effect of a jet element:

$$\delta u_s = -\frac{\bar{m}}{4\pi}\frac{X - X_p}{[(Z - Z_p)^2 + (X - X_p)^2]} \times \left[\frac{Y_p - (d/2)}{[(Z - Z_p)^2 + (X - X_p)^2 + (Y_p - d/2)^2]^{1/2}} - \frac{Y_p + (d/2)}{[(Z - Z_p)^2 + (X - X_p)^2 + (Y_p + d/2)^2]^{1/2}}\right] \tag{20}$$

$$\delta v_s = -\frac{\bar{m}}{4\pi} \times \left[\frac{1}{\{(Z - Z_p)^2 + (X - X_p)^2 + [Y_p - (d/2)]^2\}^{1/2}} - \frac{1}{\{(Z - Z_p)^2 + (X - X_p)^2 + [Y_p + (d/2)]^2\}^{1/2}}\right] \tag{21}$$

$$\delta w_s = -\frac{\bar{m}}{4\pi}\frac{(Z - Z_p)}{[(Z - Z_p)^2 + (X - X_p)^2]} \times \left[\frac{Y_p - (d/2)}{\{(Z - Z_p)^2 + (X - X_p)^2 + [Y_p - (d/2)]^2\}^{1/2}} - \frac{Y_p + (d/2)}{\{(Z - Z_p)^2 + (X - X_p)^2 + [Y_p + (d/2)]^2\}^{1/2}}\right] \tag{22}$$

From the jet geometry, we see that the strength of the doublet distribution, μ, is given by

$$\left.\begin{aligned} \mu &= \frac{\pi U d^2}{4}\cos\theta\left(1 - \frac{5}{4}\frac{Z}{d_0}\frac{U}{U_{j0}}\right) \\ & \qquad 0 \leq \frac{Z}{d_0}\frac{U}{U_{j0}} \leq 0.3 \\ \mu &= \frac{5\pi U d^2 \cos\theta}{32} \qquad \frac{Z}{d_0}\frac{U}{U_{j0}} > 0.3 \end{aligned}\right\} \tag{23}$$

With the notation of Fig. 1, the induced velocity field at a point $P(\xi,\eta,\zeta)$ due to a doublet of strength μ at $(\xi,\eta,\zeta) = (0,0,0)$ is given by

$$u_1 = -6\xi\zeta\mu/4\pi(\xi^2 + \eta^2 + \zeta^2)^{5/2} \tag{24}$$

$$v_1 = -6\eta\zeta\mu/4\pi(\xi^2 + \eta^2 + \zeta^2)^{5/2} \tag{25}$$

$$w_1 = \frac{2\mu}{4\pi(\xi^2 + \eta^2 + \zeta^2)^{3/2}}\left[1 - \frac{3\zeta^2}{\xi^2 + \eta^2 + \zeta^2}\right] \tag{26}$$

in which u_1, v_1, w_1, are the velocities in the directions (ξ, η, ζ). Now if we consider a jet element centered at $(X,0,Z)$, the induced velocities δu_B, δv_B, δw_B in the X, Y, Z directions at a point $P(X_p,Y_p,Z_p)$ are

$$\left.\begin{aligned} \delta u_B &= u_1 \sin\theta + w_1 \cos\theta \\ \delta v_B &= -v_1 \\ \delta w_B &= u_1 \cos\theta - w_1 \sin\theta \end{aligned}\right\} \tag{27}$$

in which u_1, v_1, w_1 are given by Eqs. (24–26),

$$\left.\begin{aligned} \xi &= (X_p - X)\sin\theta - (Z - Z_p)\cos\theta \\ \eta &= -Y_p \\ \zeta &= (X_p - X)\cos\theta + (Z - Z_p)\sin\theta \end{aligned}\right\} \tag{28}$$

and μ is obtained from expression (23).

The total interference velocity at a point may be determined by integrating Eqs. (20–22) and Eq. (27) over the extent of the jet giving the total induced sink and doublet component velocities. These component velocities are then summed to give the total interference velocity.

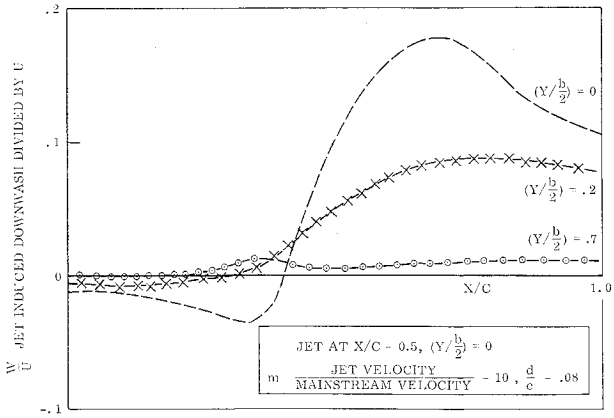

Fig. 4 Jet-induced downwash for a rectangular wing of aspect ratio 3.

Calculation of Surface Loading

The jet-induced velocity normal to a surface may be calculated using a lifting surface theory.[11] The downwash $W(X, Y)$ at a point (X,Y) on a lifting surface is equated to the wing loading $P(S)$ by the equation

$$\frac{W(X,Y)}{U} = \int_S K(X,Y,S)P(S)dS \qquad (29)$$

The integral is over the wing surface, and K is the influence function. The method used for solving Eq. (29) is to replace $P(S)$ by a circular function expansion in the chordwise direction, and an algebraic expansion in the spanwise direction. A set of downwash control points (X_c, Y_c) are chosen. The influence function $K(X,Y,S)$ and the double series expansion for $P(S)$ are then integrated, and a matrix equation deduced. This equation

$$W = DA \qquad (30)$$

equates the downwash at the control points to the loading coefficient matrix A and the influence matrix D, which is a combination of the loading and influence functions. The downwash associated with the loading must then be equal and opposite to the induced downwash from the jet to satisfy the boundary condition of no flow across the lifting surface. The induced downwash normal to a surface containing a jet is of an unusual form, as demonstrated in Fig. 4. To represent the chordwise downwash distribution satisfactorily for the solution of Eq. (30), it is necessary to use a large number of terms in the loading expansion. However, the numerical accuracy of the procedure decreases with increase in the number of loading terms. Thus it is necessary to compromise between the two requirements. It was found that seven chordwise modes and five spanwise modes gave the best representation of the downwash distribution without losing numerical accuracy.

In the method, more control points than terms in the loading series are used so that the problem is overdeterminate. The method of least squares is used to determine A so that Eq. (30) becomes

$$A = \{D^T D\}^{-1} D^T W \qquad (31)$$

From the loading coefficient matrix A, it is possible to obtain the induced velocities in the plane of the lifting surface. The velocities induced by the lifting surface are added to the velocities induced in the X direction by the jet to give the final velocity distribution on the lifting surface. It is a simple numerical computation to obtain the upper and lower surface loading from the velocity distribution. A typical chordwise loading distribution is shown in Fig. 5.

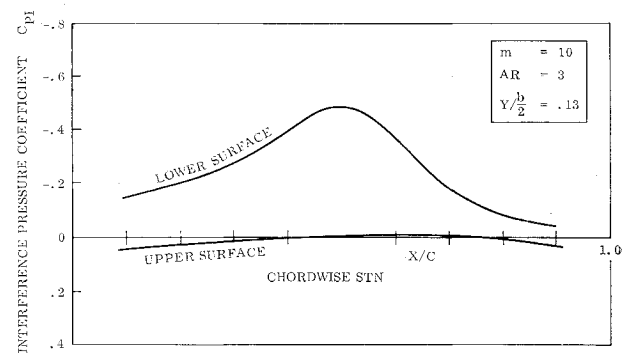

Fig. 5 Wing surface interference pressure distribution.

Experimental Investigation

The experimental part of the program was designed so that the data obtained would either verify or contradict the model of the flow used. A symmetrical, 10% thick, rectangular wing of aspect ratio 3 was chosen for the test. The air, supplied by a compressor, was passed through driers, oil filters, and then through a circular pipe with a 0.8-in.-diam nozzle. The model, having a span of 30 in., chord 10 in., was stationed in the center of the 10- × 7-ft rectangular test section of the low-speed tunnel, as shown on Fig. 6. The tunnel, designed for laminar flow tests, provided continuously variable airflow of uniform quality, the turbulence factor being 1.021.

The pressure distribution over the model was determined by cutting pressure holes in the model surface and connecting to an inclined manometer giving a scale magnification of

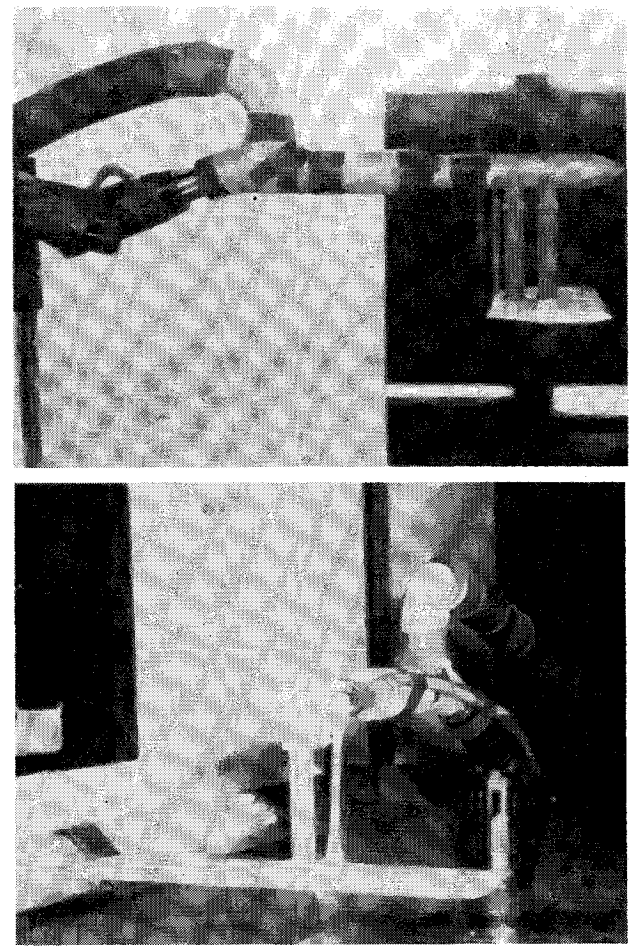

Fig. 6 Experiment arrangement.

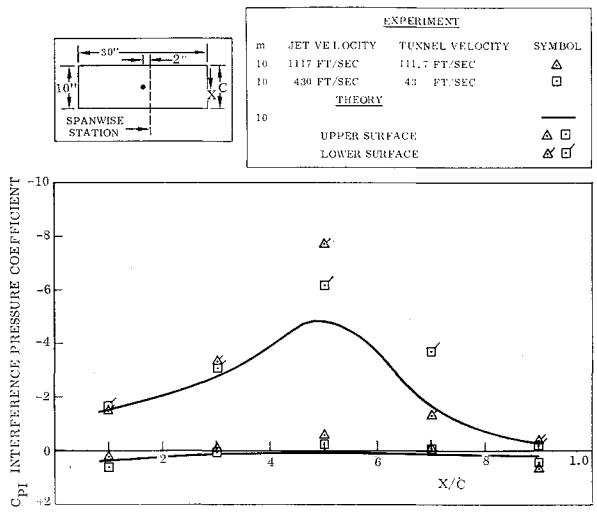

Fig. 7 Wing surface interference pressure distribution.

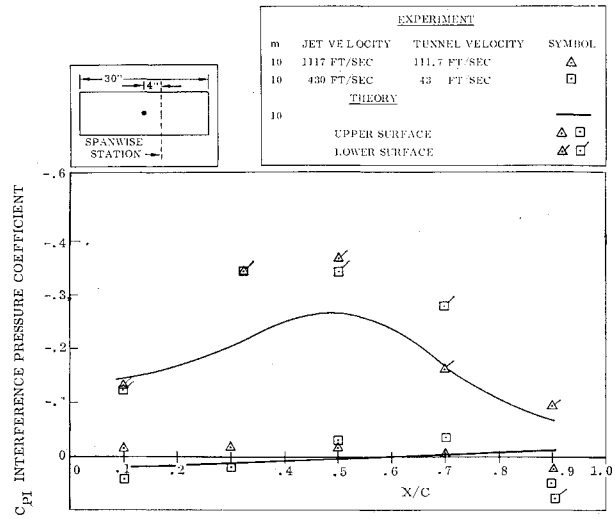

Fig. 9 Wing surface interference pressure distribution.

5. The model was placed at zero lift, this position being fixed by comparing static pressures on the upper and lower surfaces.

Two jet velocities were chosen, and the tunnel run so that the ratio of tunnel to jet velocity was the same in both cases. Static pressure measurements were taken with the tunnel running first with the jet on, and secondly with the jet off. Comparison of the two sets of data then gave the jet interference pressure field on the wing surface.

Theoretical and Experimental Results

The comparison of test data with the theoretical calculations is shown in Figs. 7–13. The upper and lower surface chordwise pressure distribution at a given spanwise station is illustrated in Fig. 7, and the loading at a spanwise station is illustrated in Fig. 8.

Linearized theory shows that the loading on a wing is distributed equally on the upper and lower surfaces of the wing. However, in the problem under discussion, a further adjustment is necessary before satisfactory correlation with test data may be expected. The reason is that besides inducing a velocity normal to the wing, the jet also induces a velocity tangential to the wing surface that may be of the same order of magnitude as the induced velocity, because of the lifting effect of the wing. Thus, although this jet-induced tangential velocity has only a minor effect on the wing loading, it may cause a significant change in the surface pressure field. That there is a significant effect is illustrated in Figs. 7 and 8. Figure 8 shows the wing loading at a spanwise station and Fig. 7 shows that this loading is not distributed equally on the upper and lower surfaces. This is accounted for in the following manner. When the jet-induced downwash is put into the lifting surface program as an effective camber, an incremental C_P distribution is obtained. This is caused by a velocity increment u induced on the upper surface and $-u$ on the lower surface, where the value of u can be computed readily from the C_P. The jet also induces a velocity component in the X direction at the wing surface, say u_j, which is the same for both upper and lower surfaces. Thus the actual loading predicted for the upper and lower surfaces is due to a velocity, $u + u_j$, on the upper surface, and $-u + u_j$ on the lower surface. The theoretical calculations taking into account the jet-induced tangential velocity are seen to agree satisfactorily with the test data.

Figures 9–12 show results for other spanwise stations, and again the agreement between theory and test data is satisfactory, showing that the theoretical calculations do account for the three-dimensionality of the problem.

Figure 13 shows the theoretical and experimental interference spanwise loading. The theoretical predictions are satisfactory, although it is noticed that the tendency is to smooth out the loading which suggests that an improvement

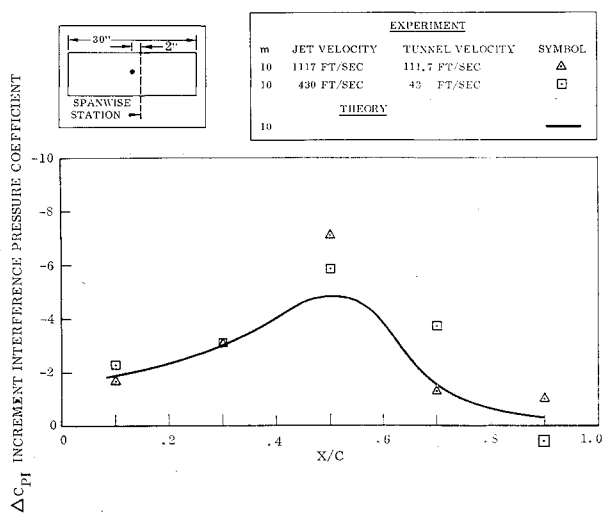

Fig. 8 Wing chordwise loading.

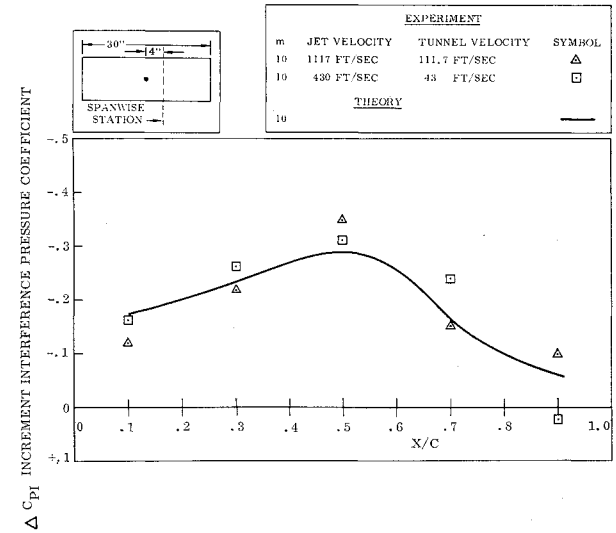

Fig. 10 Wing chordwise loading.

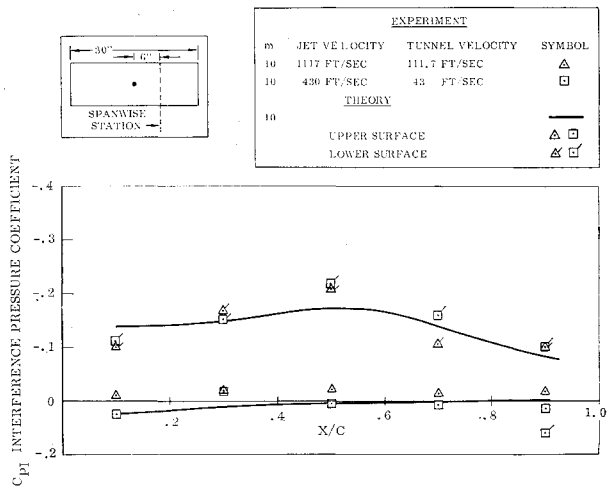

Fig. 11 Wing surface interference pressure distribution.

in the numerical procedure employed in the lifting surface program would improve the correlation.

Conclusions

1) The test data show satisfactory correlation with the theoretical calculations, both for the surface pressure coefficients and for the wing loading. The model of the flow will be very useful for determining the aerodynamic characteristics of V/STOL models.

2) An improvement in the numerical procedure involved in the lifting surface program will improve the theoretical calculations.

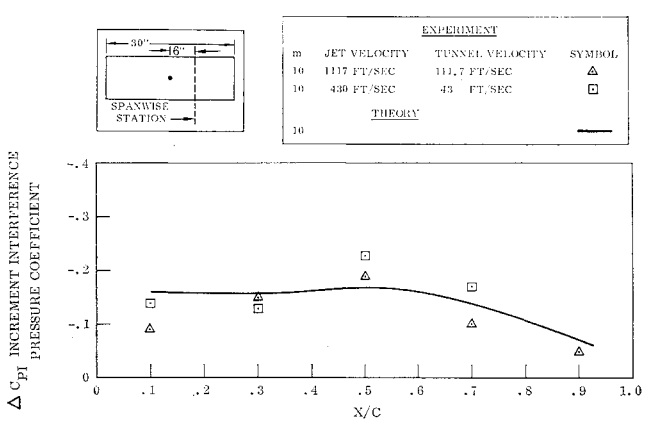

Fig. 12 Wing chordwise loading.

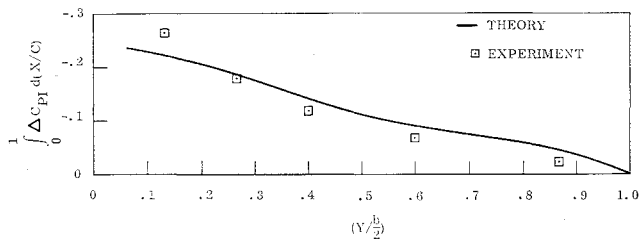

Fig. 13 Span loading distribution.

References

[1] Jordinson, R., "Flow in a jet directed normal to the wind," British Aeronautical Research Council R&M 3074(1958).

[2] Gallagher, J. T. and Williams, R., "The mixing of discrete air jets," unpublished thesis, College of Aeronautics, Cranfield (June 1959).

[3] Keffer, J. F. and Baines, W. D., "The round turbulent jet in a cross-wind," J. Fluid Mech. **15,** 481–496 (1963).

[4] Gelb, G. H. and Martin, W. A., "An experimental investigation of the flow field about a subsonic jet exhausting into a quiescent and a low velocity airstream," Northrop Corp. Rept. NOR 66-229 (1965).

[5] Bradbury, L. J. S. and Wood, M. N., "The static pressure distribution around a circular jet exhausting normally from a plane wall into an airstream," Royal Aircraft Establishment Tech. Note AERO 2978 (August 1964).

[6] Abramovich, G. N., *The Theory of Turbulent Jets* (The Massachusetts Institute of Technology Press, Cambridge, Mass., 1963).

[7] Wooler, P. T., "On the flow past a circular jet exhausting at right angles from a flat plate or wing," J. Roy. Aeronaut. Soc. **71,** 216–218 (March 1967).

[8] Monical, R. E., "A method of representing fan-wing combinations for three-dimensional potential flow solutions," J. Aircraft **2,** 527–530 (1965).

[9] Ricou, F. P. and Spalding, D. B., "Measurements of entrainment by axisymmetrical turbulent jets," J. Fluid Mech. **II,** 25–32 (1961).

[10] Milne-Thomson, L. M., *Theoretical Hydrodynamics* (The Macmillan Co., New York, 1963).

[11] Stevens, J. R. and McDonald, J. W., "Subsonic lifting surface theory design and analysis procedure," Northrop Corp. Rept. NOR 64-195 (April 1965).